Establishment of Patient-Derived Non–Small Cell Lung Cancer Xenografts as Models for the Identification of Predictive Biomarkers

Iduna Fichtner,[1] Jana Rolff,[1] Richie Soong,[3] Jens Hoffmann,[4] Stefanie Hammer,[4] Anette Sommer,[4] Michael Becker,[5] and Johannes Merk[2]

Abstract

Purpose: It was the aim of our study to establish an extensive panel of non-small cell lung cancer (NSCLC) xenograft models useful for the testing of novel compounds and for the identification of biomarkers.

Experimental Design: Starting from 102 surgical NSCLC specimens, which were obtained from primarily diagnosed patients with early-stage tumors (T_2/T_3), 25 transplantable xenografts were established and used for further investigations.

Results: Early passages of the NSCLC xenografts revealed a high degree of similarity with the original clinical tumor sample with regard to histology, immunohistochemistry, as well as mutation status. The chemotherapeutic responsiveness of the xenografts resembled the clinical situation in NSCLC with tumor shrinkage obtained with paclitaxel (4 of 25), gemcitabine (3 of 25), and carboplatin (3 of 25) and lower effectiveness of etoposide (1 of 25) and vinorelbine (0 of 11). Twelve of 25 NSCLC xenografts were >50% growth inhibited by the anti-epidermal growth factor receptor (EGFR) antibody cetuximab and 6 of 25 by the EGFR tyrosine kinase inhibitor erlotinib. The response to the anti-EGFR therapies did not correlate with mutations in the EGFR or p53, but there was a correlation of K-ras mutations and erlotinib resistance. Protein analysis revealed a heterogeneous pattern of expression. After treatment with cetuximab, we observed a down-regulation of EGFR in 2 of 6 sensitive xenograft models investigated but never in resistant models.

Conclusion: An extensive panel of patient-derived NSCLC xenografts has been established. It provides appropriate models for testing marketed as well as novel drug candidates. Additional expression studies allow the identification of stratification biomarkers for targeted therapies.

Clinical trials in non-small cell lung cancer (NSCLC) patients with therapies targeting the epidermal growth factor receptor (EGFR) have been accompanied with great expectations but have thus far shown only limited achievement compared with chemotherapy (1–5). Several different reasons for the insufficient responses of anti-EGFR therapies, be it anti-EGFR antibodies or EGFR tyrosine kinase inhibitors (TKI), have been discussed such as changes in the EGFR gene or protein itself (amplification, mutations, and overexpression), constitutive expression of ligands, dysregulation of pathways downstream of the EGFR (6), or involvement of ABC transporters in case of small-molecule EGFR inhibitors (7). Main focus has been given to the analysis of mutations in the EGFR and their effect on drug responses (8, 9). It was elucidated that mutations can either be associated with drug sensitivity or drug resistance toward small-molecule EGFR inhibitors. An association between mutations (small in frame deletions or substitutions) in the EGFR tyrosine kinase domain encoded by exons 18 to 21 with hyperresponse to gefitinib were mainly found in females, patients of Asian origin, never-smokers, and a subtype of adenocarcinomas (10–12). Additional mutations in the *K-ras* and the *p53* gene have been reported to contribute to response of NSCLC to EGFR-targeted TKI (13, 14).

The ability of cancer cells to activate key downstream signaling pathways regardless of upstream inhibition, most notably the phosphoinositide 3-kinase/AKT pathway, was further discussed as potential resistance mechanism. Several redundant signaling pathways exist. One mechanism of redundancy leading to resistance includes focal amplification of the *c-Met* proto-oncogene. Inhibition of c-Met signaling could restore sensitivity to EGFR TKI (gefitinib; ref. 15). One further critical signaling pathway that is down-regulated on successful treatment with EGFR1 TKI is the phosphoinositide 3-kinase signaling pathway. There are several reports suggesting that the phosphoinositide 3-kinase/AKT signaling pathway is also central to NSCLC growth and survival (16).

Authors' Affiliations: [1]Max Delbrück Center for Molecular Medicine; [2]Evangelische Lungenklinik; [3]National University of Singapore, Singapore; [4]Bayer Schering Pharma AG, Berlin, Germany; and [5]Experimental Pharmacology and Oncology GmbH, Berlin-Buch, Germany

Received 1/18/08; revised 5/23/08; accepted 5/29/08.

The costs of publication of this article were defrayed in part by the payment of page charges. This article must therefore be hereby marked *advertisement* in accordance with 18 U.S.C. Section 1734 solely to indicate this fact.

Note: Supplementary data for this article are available at Clinical Cancer Research Online (http://clincancerres.aacrjournals.org/).

Requests for reprints: Iduna Fichtner, Max Delbrück Center for Molecular Medicine, Robert-Rössle-Str. 10, 13125 Berlin-Buch, Germany. Phone: 49-309-4062295; Fax: 49-309-4063823; E-mail: Fichtner@mdc-berlin.de.

doi:10.1158/1078-0432.CCR-08-0138

Translational Relevance

In this article, the establishment of patient-derived xenografts is described. These models show a high concordance with the clinical samples concerning histology and gene and protein expression. Therefore, they can be used for individual testing of responsiveness toward clinically used therapies. Further on, they allow the identification of biomarkers as a precondition for the use of novel targeted therapies. The procedure and the methods described here for NSCLC can serve as example for other tumor types. Compared with clinical specimens used frequently for the identification of biomarkers, xenografts are more homogeneous, supply sufficient material for analyses on protein level, and allow the study of dynamic regulations under standardized conditions. Concerning the intended identification of biomarkers for EGFR-targeted therapies, our results reveal a lack of correlation to EGFR and p53 mutations but confirm the relative importance of K-ras mutations for the resistance phenotype. These data can directly support clinical decisions concerning the stratification of patients with NSCLC to be treated with cetuximab or erlotinib.

It is beyond doubt that an adequate stratification of patients to be treated with targeted therapies is mandatory but unfortunately is not routinely available at present (17). Therefore, comprehensive searches for predictive biomarkers trying to define genes or proteins with therapeutic relevance are currently pursued. These studies use mainly clinical samples (18, 19), cell lines (20, 21), or cell-line derived xenograft models (20, 22–25). Only few groups report on patient-derived xenografts (26–28).

We were able to establish an extensive panel of NSCLC xenograft models that were derived from early-stage T_2 and T_3 tumors of primarily diagnosed patients. The clinical samples and the early passages of the xenograft tissue on nude mice were investigated by gene expression arrays as well as histologic and immunohistochemical methods. A further goal of our investigations was to find a potential correlation of responses of anti-EGFR therapies with mutations in the EGFR or the expression of proteins involved in EGFR-related signaling pathways.

Materials and Methods

Patients and tissue samples

One hundred and two tumor specimens were obtained at initial surgery from primarily diagnosed, early-stage NSCLC patients between July 2004 and January 2007. Written informed consent was obtained from each patient and the study was approved by the local ethical committee. From these samples, 25 passagable xenograft models were successfully established, which were analyzed in the study described here (Table 1). Four of the 25 patients had received chemotherapy or radiation therapy before surgery. The histologic type was determined according to WHO criteria. The collective consisted of 12 (48%) squamous cell carcinomas, 6 (24%) adenocarcinomas, and 4 (16%) carcinomas with a pleiomorphic phenotype. The remaining tumors were diagnosed as large-cell or dedifferentiated carcinomas, and one tumor was secondarily defined as small-cell lung carcinoma. The samples originated from 12 (44%) female and 13 (56%) male patients. With one exception (SQC 7298), the patients were long-term smokers. Pathologic staging was determined according to Mountain (29). All of the tumor samples were put into medium immediately after surgical resection under sterile conditions and transported without delay to the animal facility.

Establishment of xenografts

Surgical tumor samples were cut into pieces of 3 to 4 mm and transplated within 30 min s.c. to 3 to 6 immunodeficient NOD/SCID mice (Taconic); the gender of the mice was chosen according to the donor patient. Additional tissue samples were immediately snap-frozen and stored at -80°C for genetic, genomic, and protein analyses. All animal experiments were done in accordance with the United Kingdom Co-ordinating Committee on Cancer Research regulations for the Welfare of Animals and of the German Animal Protection Law and approved by the local responsible authorities. Mice were observed daily for tumor growth. At a size of about 1 cm^3, tumors were removed and passaged to naive NMRI:*nu*/*nu* mice (Charles River) for chemosensitivity testing. Tumors were passaged no more than 10 times. Numerous samples from early passages were stored in the tissue bank in liquid nitrogen and used for further experiments. Several rethawings led to successful engraftment in nude mice.

Chemosensitivity testing

The chemotherapeutic response of the passagable tumors was determined in male NMRI:*nu*/*nu* mice. For that purpose, one tumor fragment each was transplanted s.c. to a large number of mice. At palpable tumor size (50-100 mm^3), 6 to 8 mice each were randomized to treatment and control groups and treatment was initiated. If not otherwise mentioned, the following drugs and treatment modalities were used: etoposide (Vepesid; Bristol-Meyers Squibb) 10 mg/kg/d, qd 1-5, i.p.; carboplatin (Mayne Pharma Deutschland) 75 mg/kg/d, qd 1 and 8, i.p.; gemcitabine (Gemzar; Lilly Deutschland) 60-80 mg/kg/d, qd 1, 4, 7, and 10, i.p.; paclitaxel (Taxol; Sigma) 12.5 mg/kg/d, qd 1-5, i.v.; vinorelbine (Navelbine; Pierre Fabre Pharma) 1-5 mg/kg/d qd 1 and 8, i.p.; cetuximab (Erbitux; Merck) 50 mg/kg/d, qd 1-5, i.p.; and erlotinib (Tarceva; Hoffmann-LaRoche) 50 mg/kg/d, qd 1-5 and 8-12, p.o. Doses and schedules were chosen according to previous experience in animal experiments and represent the maximum tolerated or efficient doses. The injection volume was 0.2 mL/20 g body weight.

Tumor size was measured in two dimensions twice weekly with a caliper-like instrument. Individual tumor volumes (V) were calculated by the formula: $V = (\text{length} + [\text{width}]^2) / 2$ and related to the values at the first day of treatment (relative tumor volume). Median treated to control (T/C) values of relative tumor volume were used for the evaluation of each treatment modality and categorized according to scores (- to ++++; see Tables 2 and 3). The mean tumor doubling time of each xenograft model was calculated by comparing the size between 2- and 4-fold relative tumor volumes. Statistical analyses were done with the U test (Mann and Whitney) with $P < 0.05$. The body weight of mice was determined every 3 to 4 days and the change in body weight was taken as variable for tolerability.

Mutational analysis

DNA extraction. Genomic DNA was isolated from xenograft samples with the QIAamp DNA Mini Kit (Qiagen) according to the manufacturer's instructions. DNA was quantified spectrophotometrically using the ND-100 (Nanodrop).

EGFR and p53 mutation analysis. Mutations in the tyrosine kinase domain (exons 18-21) of EGFR and exons 5 to 9 of p53 were detected with partially denaturing high-performance liquid chromatography as described previously (30, 31).

DNA sequencing. PCR products were purified with 2 μL ExoSAP-IT reagent (USB Corporation) at 37°C for 15 min followed by inactivation at 80°C for 15 min. Direct sequencing using BigDye Terminator version

3.1 Cycle Sequencing Kit (Applied Biosystems) was done on the 3100*xl* Genetic Analyzer (Applied Biosystems) following manufacturer's instructions. All variants were sequenced bidirectionally.

K-ras mutation analysis. Samples were screened for all types of mutations in K-ras codons 12 and 13 by pyrosequencing as described previously (32).

Genome-wide gene expression analysis

RNA extraction. RNA was extracted from NSCLC specimens and from $2 \times 2 \times 2$ mm^3 tumor xenograft samples (derived from different passages ranging from 1 to 6), which were taken from the sacrificed animals. Samples were snap-frozen and stored in liquid nitrogen until use. Total RNA of homogenized tumor samples was prepared with Trizol RNA extraction reagent (Invitrogen) followed by purification using the RNeasy Mini Kit (Qiagen) according to the manufacturer's recommendations. A DNase I (Qiagen) digestion step was included to eliminate genomic DNA. The quality of the total RNA was checked for integrity using RNA LabChips on the Agilent Bioanalyzer 2100 (Agilent Technologies) and the concentration was measured on the Peqlab NanoDrop. Only RNA with a RNA integrity number larger than 6.5 was used for cDNA synthesis.

Array hybridization. The one-cycle eukaryotic target labeling assay from Affymetrix was used according to manufacturer's instructions. Briefly, 2 μg high-quality total RNA was reverse transcribed using T7-tagged oligo-dT primer in the first-strand cDNA synthesis reaction. After RNase H-mediated second-strand cDNA synthesis, the double-stranded cDNA was purified and served as template for the subsequent in vitro transcription reaction, which generates biotin-labeled cRNA. The biotinylated cRNA was cleaned up, fragmented, and hybridized to GeneChip HGU133Plus2.0 expression arrays (Affymetrix), which contain 54,675 probe sets. The GeneChips were washed and stained with streptavidin-phycoerythrin on a GeneChip Fluidics Station 450 (Affymetrix). After washing on a GeneChip Fluidics Station 450, the arrays were scanned on an Affymetrix GeneChip 3000 scanner with autoloader and barcode reader (Affymetrix).

Data analysis. The quality of the hybridized arrays was analyzed with the Expressionist Pro 4.0 Refiner (GeneData) software. Here, based on raw intensities of individual oligonucleotide features (probes), the following analyzes are done: the experiments are grouped according to similarity and potential outlier experiments can be removed (or selected for rehybridization or refragmentation), and the quality of a particular experiment is compared with a virtual reference experiment, which is computed as average of all feature intensities of all arrays in that group. Moreover, defects on the arrays are masked. Here, for each array, the spatial signal distribution is compared with the reference experiment of the experiment group it belongs to. Regions with sharp boundaries, which have consistently higher or lower feature intensities compared with the reference experiment, are flagged as defects and excluded from further analysis. In addition, a signal correction (distortion and gradient) is done, the control gene statistics are calculated, and an overall classification of the quality of the experiments is provided. The probe intensities on each array were summarized with the MAS5.0 summarization algorithm and the refined and summarized data were loaded into the CoBi database (GeneData). The analysis of the probe set-specific signal intensities was done with the Expressionist Pro 4.0 Analyst (GeneData) software. The data set was median-normalized.

Hierarchical clustering of all experiments was done based on all probe sets represented on the HGU133Plus2.0 array with a quality $P < 0.04$ using positive correlation and complete linkage. Gene expression of primary tumors was compared with the median arrays of replicate tumors from each xenograft model in a paired *t* test. Probe sets differentially expressed at a $P < 10^{-7}$ were subjected to pathway analysis using Metacore software (GeneGo).

Profiling human genes expressed in human NSCLC-derived xenograft models on nude mice using the human-specific Affymetrix array HGU133Plus2.0 will mostly uncover genes specifically expressed in human cancer cells in xenograft tumors composed of a mixture of human- and mouse-derived cells. Using the human-specific Affymetrix arrays in contrast to cDNA arrays has the advantage that

Table 1. Clinical and pathologic characteristic of passagable lung cancer

ID	Age	Sex	Smoker	Tumor-stage	Prior treatment
PLC 7064	69	F	Since 9 y n-s	pT_3 pN_0 M_0 G3 R0	No
SQC 7126	42	F	s	pT_3 pN_0 cM_0 G2 R0	Cisplatin/vinorelbine
LCC 7166	70	M	Since 11 y n-s	pT_2 pN_2 cM_0 G3 R0	No
SQC 7177	42	M	s	ypT_2 ypN_2 cM_0 G3 R0	5 cycles carboplatin/paclitaxel
PLC 7187	38	F	s	pT_3 pN_0 cM_0 G3 R0	No
ADC 7198	60	F	s	pT_2 pN_0 cM_0 G3 R0	No
SQC 7298	73	M	n-s	pT_2 pN_2 cM_0 G3 R1	No
PLC 7336	79	M	s	pT_2 pN_1 cM_0 G3 R1	No
SQC 7343	52	F	s	pT_3 pN_0 cM_0 G3 R1	No
ADC 7387	55	M	s	$T_xN_2pM_1$	No
ADC 7406	53	F	s	ypT_2 ypN_2 cM_0 G3 R0	2 cycles cisplatin/vinorelbine
SQC 7414	64	M	s	pT_2 pN_0 cM_0 G3 R0	No
SQC 7433	72	M	s	pT_3 pN_2 cM_0 G3 R0	No
ADC 7462	55	F	s	pT_3 pN_0 cM_0 G3 Rx	No
ADC 7466	57	M	s	pT_2 pN_1 cM_0 G3 R0	No
SQC 7506	70	F	s	pT_2 pN_1 pM_1 G3 R0	No
SCLC 7530	69	M	Since 5 y n-s	ypT_2 ypN_1 cM_0 G3 R0	2 cycles carboplatin/etoposide
PLC 7558	74	M	Since 11 y n-s	pT_4 pN_1 cM_0 G3 R0	No
SQC 7612	51	M	s	pT_3 pN_0 cM_0 G3 R0	No
DDC 7668	66	F	s	pT_2 pN_0 cM_1 G4 R0	No
ADC 7700	44	F	s	ypT_1 ypN_2 cM_0 G2 R0	No
SQC 7747	73	F	s	pT_3 pN_0 cM_0 G2 R0	No
SQC 7766	71	M	Since 20 y n-s	pT_2 pN_2 cM_0 G3 R0	No
SQC 7860	71	M	Since 20 y n-s	pT_1 pN_0 cM_0 G3 R0	No
SQC 7913	58	F	s	pT_2 pN_2 cM_0 G2 R1	No

Abbreviations: M, male; F, female; n-s, nonsmoker; s, smoker; ADC, adenocarcinoma; DDC, dedifferentiated carcinoma; LCC, large cell carcinoma; PLC, pleiomorphic carcinoma; SQC, squamous cell carcinoma; SCLC, small cell lung cancer.

Table 2. Chemotherapeutic responsiveness

ID	TDT ± SD (d)	Etoposide	Carboplatin	Gemcitabine	Paclitaxel	Vinorelbine
PLC 7064	17.2 ± 4.6	++	-	-	++	-
SQC 7126	12.1 ± 4.2	-	-	+++	-	-
LCC 7166	19.5 ± 18.5	++	++	+	-	-
SQC 7177	9.5 ± 1.7	-	++	+++	-	-
PLC 7187	11.1 ± 2.0	-	++	+++	-	++
ADC 7198	19.2 ± 1.6	-	+	+	+	+
SQC 7298	8.4 ± 3.8	+	+	++	++	+
PLC 7336	15 ± 5.8	-	(+)	++	+++	n.t.
SQC 7343	9.1 ± 1.4	-	+++	+++	++	-
ADC 7387	8.9 ± 1.8	-	-	+++	++++	+
ADC 7406	10.4 ± 1.9	+	+	+++	+++	-
SQC 7414	7.2 ± 2.1	-	++	+++	+++	n.t.
SQC 7433	11.7 ± 6.2	-	+++	-	++++	n.t.
ADC 7462	5.2 ± 0.3	-	+	++++	+++	n.t.
ADC 7466	5.8 ± 1.5	-	-	++++	++++	-
SQC 7506	10.7 ± 3.7	-	++++	(+)	+++	n.t.
SCLC 7530	8.4 ± 1.9	++++	-	tox	+++	n.t.
PLC 7558	11.2 ± 3.0	-	++++	+++	-	n.t.
SQC 7612	9.7 ± 1.6	-	++++	-	+++	n.t.
DDC 7668	10.1 ± 7.2	-	+++	tox	++++	n.t.
ADC 7700	14.1 ± 5.1	-	-	++++	++	n.t.
SQC 7747	9.5 ± 2.5	-	++	-	++	n.t.
SQC 7766	12.8 ± 7.5	-	+++	+	++	n.t.
SQC 7860	20.4 ± 6.0	+	-	++	+++	n.t.
SQC 7913	7.8 ± 1.9	-	+	(+)	+++	n.t.
TS		1/25	3/25	3/25	4/25	0/11
STD		5/25	15/25	16/25	16/25	4/11
RR		6/25	18/25	19/25	20/25	4/11

NOTE: Groups of 6 to 8 tumor-bearing mice were treated with the maximum tolerated dose of the clinically used chemotherapeutics and the therapeutic response was determined. Tumor response score: - negative: 100-50% T/C; +, 35-50% T/C; ++, 21-35% T/C; +++, 6-20% T/C; ++++, 0-5% T/C; TS, tumor shrinkage (T/C 0-5%); SD, standard division; STD, stable disease (T/C 6-50%); RR, response rate (TS + STD); n.t., not tested; (+), borderline; tox, >50% toxic deaths; TDT, tumor doubling time in days measured in vehicle-treated controls.

11 independent probes as perfect match oligonucleotides interrogate a particular gene. Unless a murine gene is 100% homologous to a human gene, this provides very high specificity compared with a continuous stretch of DNA on a cDNA array. In addition, the presence of a set of 11 mismatch oligonucleotides provides a further degree of specificity as only those probe sets are incorporated in the determination of a condensed signal intensity for which perfect match > mismatch. From histologic analyses of lung cancer xenografts, the amount of murine tissue in a human lung cancer xenograft tumor was estimated to be as low as 5% to 10%.[6]

Real-time PCR

cDNA was reverse transcribed using SuperScript III Reverse Transcription Kit (Invitrogen) and TaqMan quantitative real-time PCR done using cDNA corresponding to 25 ng RNA/reaction. Gene- and species-specific primer/probe pairs for COL3A1 and GAPDH and TaqMan Fast MasterMix obtained from Applied Biosystems were used according to the manufacturer's instructions and amplifications were carried out on the Applied Biosystems 7500 Real-time PCR system with 40 cycles. Results from analysis done in duplicates are shown as mean 40 - average C_T value. For samples with no detectable signal, C_T values were set to 40, so the results are displayed as 0.

Immunoblotting

Lysates for immunoblotting were prepared by adding lysis buffer [150 mmol/L NaCl, 20 mmol/L Tris, 1% Triton X-100, 0.5% sodium deoxycholate, 0.5% SDS, 2 mmol/L EDTA, 2.5 mmol/L sodium pyrophosphate, 1 mmol/L β-glycerophosphate (pH 7.7)] containing protease and phosphatase inhibitors (Sigma-Aldrich) to the tumor tissue homogenized in fluid nitrogen. The protein concentration was determined using Bio-Rad Protein Assay (Bio-Rad Laboratories). Tumor lysates (30 μg) were separated on 9% SDS-PAGE polyacrylamide gels and transferred to nitrocellulose membranes. Membranes were blocked and incubated with the primary antibodies overnight at 4°C. The secondary antibody (DAKO) was conjugated with horseradish peroxidase. Protein bands were visualized using the enhanced chemiluminescence detection system (GE Health Amersham Life Science). To show equal protein loading, the blots were stripped and reprobed for β-actin. As positive controls for the detection of phosphorylated proteins, lysates of A431 cells treated with EGF were used (Biosciences PharMingen).

The following antibodies were used for immunoblotting: AKT was purchased from Stressgen Bioreagents; pAKT (Ser^{473}), PTEN (clone 138G), pPTEN (clone 44A7), STAT3, and pSTAT3 (Tyr^{705}, clone D3A7) from Cell Signaling (New England Biolabs); EGFR (clone 1005) from Santa Cruz Biotechnology; pEGFR (clone 74), ERK (clone MK12), pERK1/2, phosphotyrosine (clone PY69), STAT1 (clone 1), and pSTAT1 (Tyr^{701}, clone 4a) from Biosciences PharMingen; β-actin (clone AC-15) from Sigma; and swine anti-rabbit and rabbit anti-mouse antibodies from DAKO.

Results

Engraftment of xenografts. A total of 102 tumor specimens were transplanted to immunodeficient mice. From these, 25 passagable xenograft lines were obtained (Table 1). The successful growth in mice was not dependent on the clinicopathologic

[6] Fichtner et al., unpublished observations.

characteristics mentioned. Both stage T_2 and T_3 and adenocarcinomas (6 of 25) and squamous carcinomas (12 of 25) were successfully engrafted. The growth rate of the established xenografts (depicted in Table 2 as tumor doubling time) was a unique feature of the different models and not related to any patient characteristic or to the tumor type. A comparison of the H&E-stained original sample with xenografted tumors after few passages revealed the same histologic architecture of the primary NSCLC and the xenograft tumor (data not shown). The staining with the anti-EpCAM or Ki-67 antibodies revealed comparable pictures (not shown). In general, the tumors revealed a more homogeneous structure during murine passaging due to the

Table 3. Mutation analysis of xenograft models and response to EGFR inhibitors

ID	*EGFR*	*K-ras*	*p53*	Cetuximab response (score and T/C value)	Erlotinib response (score and T/C value)
PLC 7064	wt	wt	162B:del13bp (frshift>STOP)	+++	++
				17*	27*
SQC 7126	wt	wt	wt	+++	++
				19*	33*
LCC 7166	wt	wt	wt	-	-
				75	77
SQC 7177	wt	wt	M246V	-	++
				52	28*
PLC 7187	wt	G12C	wt	++	-
				27*	78
ADC 7198	IVS18+19; IVS18+73	G12C	wt	-	-
				73	63
SQC 7298	wt	wt	Y234C	+	-
				43*	54
PLC 7336	Q787Q, A836R †	G12D	P190L	-	-
				62	67
SQC 7343	wt	wt	wt	-	-
				86	57
ADC 7387	wt	wt	wt	-	-
				67	62
ADC 7406	wt	wt	P278T	-	-
				74	68
SQC 7414	wt	wt	wt	+	+
				34*	41*
SQC 7433	R836R silent	wt	258E>STOP	-	-
				88	97
ADC 7462	wt	G12C	G245V	++++	++++
				0*	1*
ADC 7466	wt	wt	R196P	++++	++
				2*	26*
SQC 7506	wt	wt	190:del1bp	+	-
				41*	95
SCLC 7530	wt	G12D, G13D	wt	-	-
				37	50
PLC 7558	Q787Q	wt	I232F	+	-
				45*	79
SQC 7612	wt	wt	wt	-	-
				85	94
DDC 7668	wt	wt	wt	++++	-
				1*	71
ADC 7700	wt	wt	H193Y	-	-
				67	109
SQC 7747	wt	wt	wt	-	-
				50	76
SQC 7766	Q787Q silent	G12D, G13D	M246K	++	-
				25*	66
SQC 7860	Q787Q silent	wt	V153F	-	-
				46	63
SQC 7913	wt	wt	wt	+++	-
				9*	59
Mutation rate	6/25	6/25	13/25		
TS				3/25	1/25
STD				9/25	5/25
RR				12/25	6/25

NOTE: Tumor response score: see Table 2; corresponding optimum (lowest) T/C values (%) are mentioned. TS, STD, and RR: see Table 2.
*Significant to vehicle (PBS)-treated control.
† Only in the forward direction a mutation was detected. IVS, intronic variation sequence.

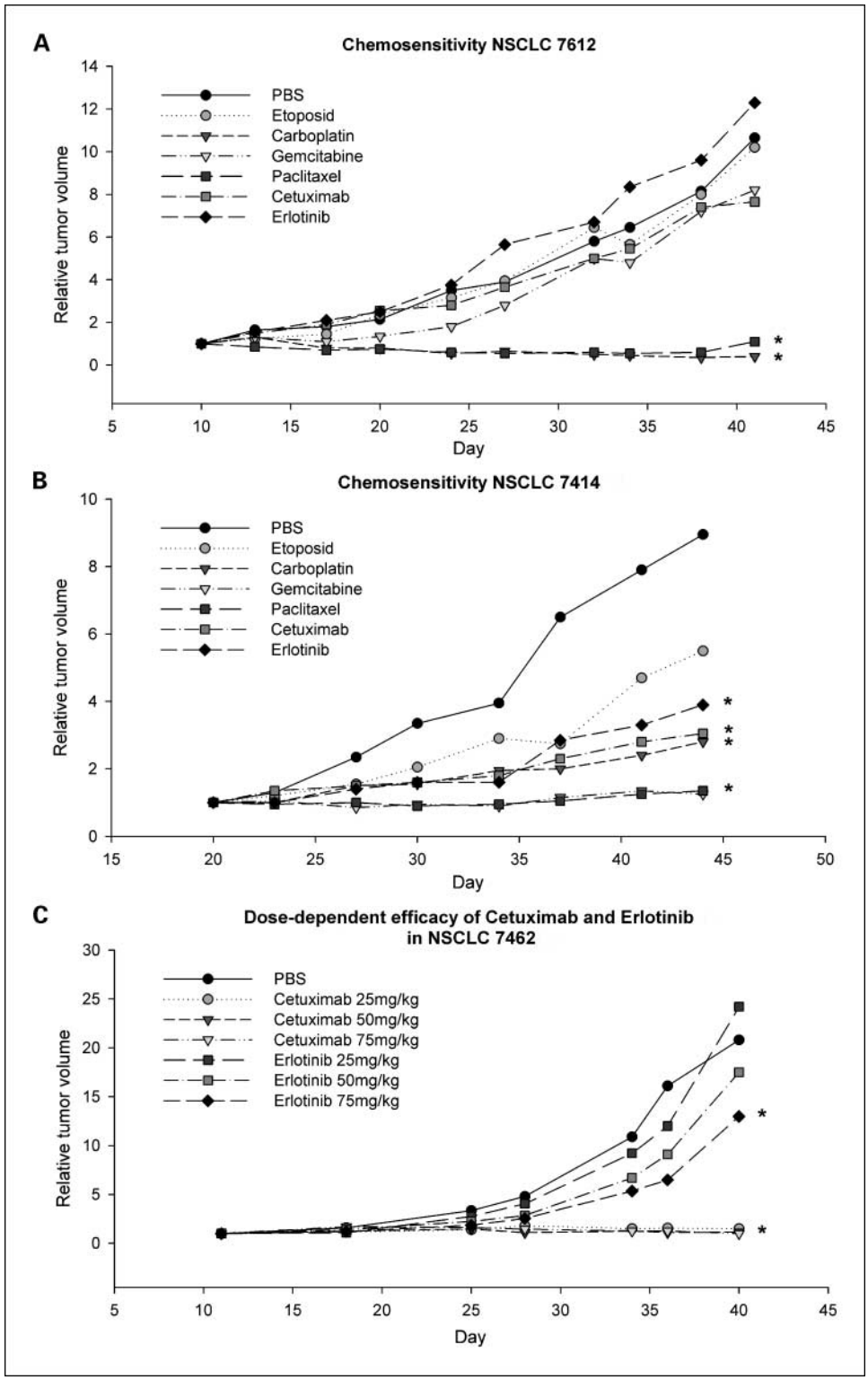

Fig. 1. Chemoresponsiveness of NSCLC xenografts. *A,* chemosensitivity of ADC 7612. *B,* chemosensitivity of squamous cell carcinoma 7414. *C,* dose-response curve of cetuximab and erlotinib in squamous cell carcinoma 7462. Six to 8 mice per group were treated with the corresponding agent according to Materials and Methods. Tumor growth was measured twice per week and blotted against time. SDs are not shown because of better clarity. *Asterisks,* significance compared with solvent-treated control.

replacement of human accessory cells (fibroblasts, endothelial, and immune cells) by murine tissues (data not shown). After two to four passages in mice, the composition of the xenograft tissue did not change any further. At that stage, xenograft transplants were archived in the tumor bank, if required retransplanted and used for chemosensitivity testing, mutation analysis, and RNA and protein analyses.

Chemosensitivity. To further characterize the established xenograft models, extensive therapeutic experiments with five cytotoxic agents, used also in the clinic for treatment of NSCLC, were done. Table 2 gives an overview on the results obtained and Fig. 1 presents exemplified growth curves of three models after different treatments. Paclitaxel, gemcitabine, and carboplatin proved to be the most efficient agents in NSCLC

xenografts with 4 of 25, 3 of 25, or 3 of 25 xenografts responding with tumor shrinkage. Etoposide (1 of 25 complete remission) and vinorelbine (0 of 11 complete remission) were less efficient.

It became obvious that some models had a high responsiveness toward the majority of agents tested (e.g., SQC 7343 and ADC 7462), whereas others were intrinsically resistant toward a variety of drugs (e.g., PLC 7064 and ADC 7198). In general,

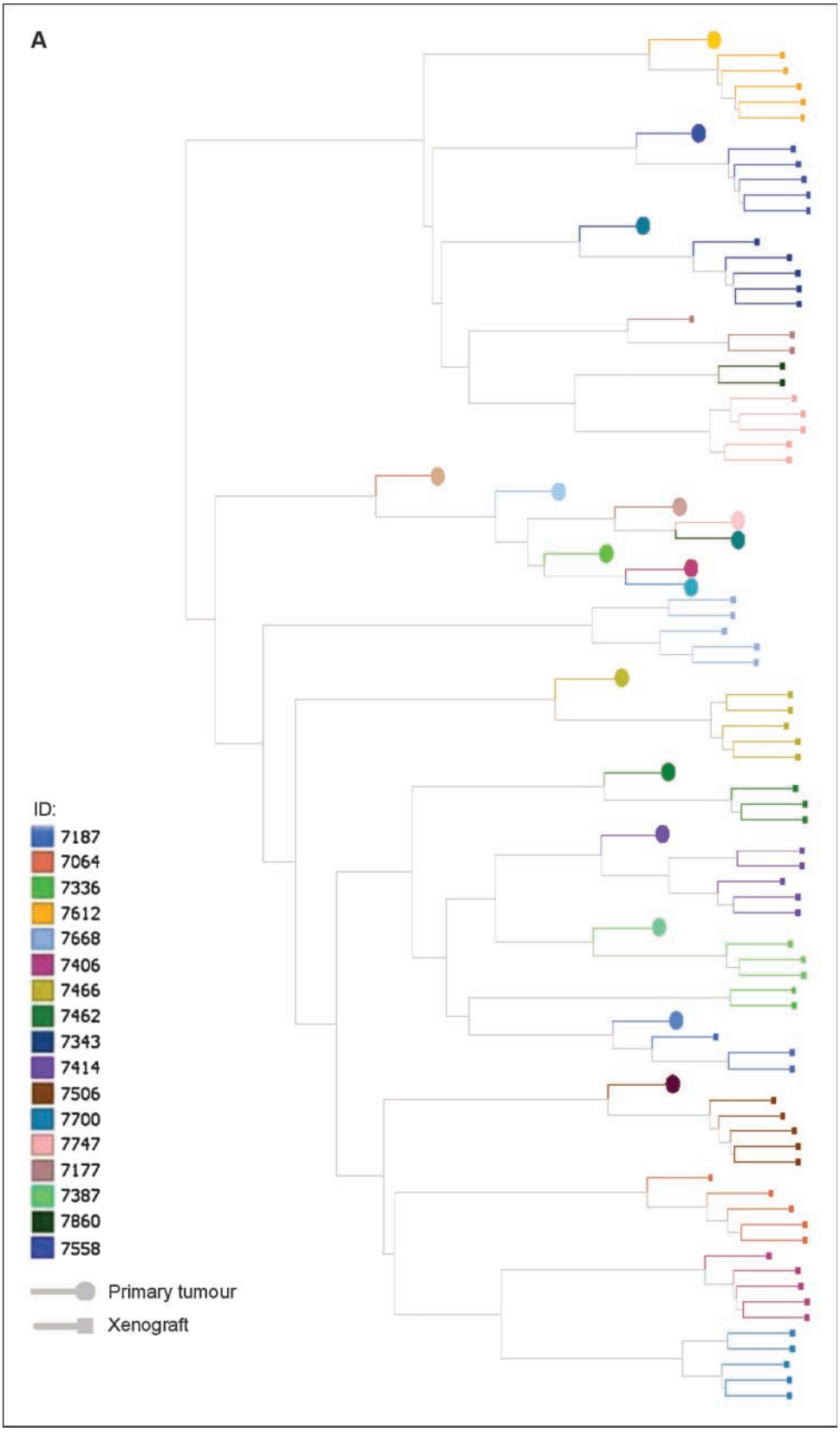

Fig. 2. Gene expression profiling of clinical lung cancer specimens and corresponding xenografts. *A,* hierarchical clustering of gene expression data from primary lung cancers and xenografts based on all probe sets (positive correlation, complete linkage) color-coded according to xenograft code.

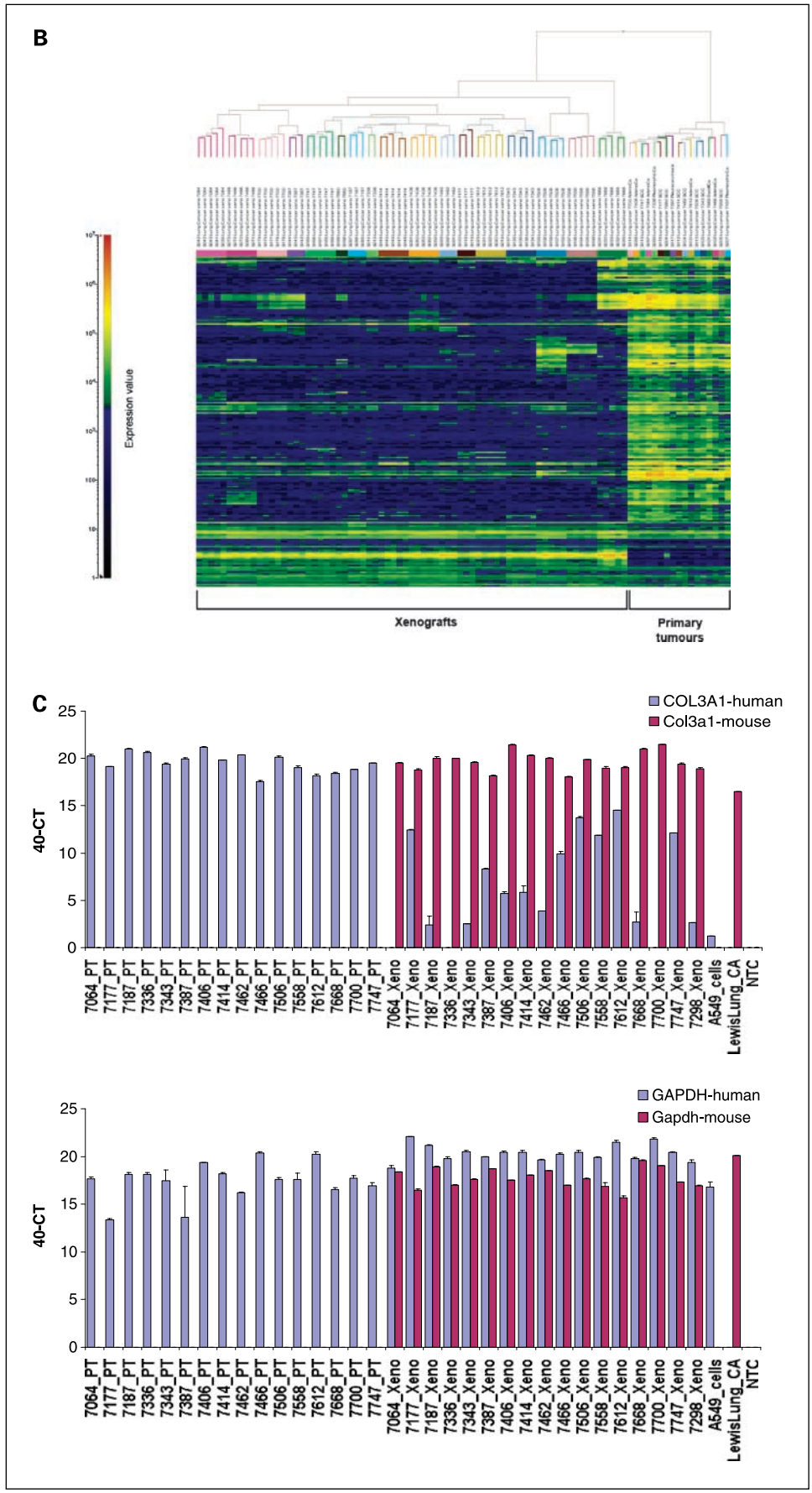

Fig. 2 *Continued. B,* two-dimensional hierarchical clustering based on 193 probe sets differentially expressed between clinical NSCLC specimens and xenograft tumors color-coded according to xenograft code. *C,* TaqMan quantitative real-time PCR with primer/probe pairs specific for human and murine COL3A1 (*top*) and GAPDH (*bottom*) transcripts.

each tumor had its individual pattern of response to the agents tested, which was independent of the tumor type (e.g., adenocarcinoma or squamous cell carcinoma). A correlation analysis comparing overall sensitivity of xenografts with their tumor doubling time revealed a higher responsiveness of models with faster growth rate (r = 0.591). Table 3 gives an overview on the responsiveness of the xenograft models to anti-EGFR therapies. Twelve of 25 models tested showed significant responses to cetuximab (3 of 25 tumor shrinkage) and 6 of 25 to erlotinib (1 of 25 tumor shrinkage). The response rates were quite different among the tumors tested, ranging from no response (~100% T/C in models ADC 7700 and SQC 7612) to complete remissions (~0% T/C in models ADC 7462 to both anti-EGFR therapies and DDC 7668 to cetuximab). The responses to anti-EGFR therapies were not related to the histologic type of NSCLC or clinical variables. Interestingly, there was a clear dose-response effect to erlotinib between 25 and 75 mg/kg, whereas this was not obvious for cetuximab (Fig. 1C). One model (SQC 7177) was moderately sensitive to erlotinib (T/C 28%) but resistant to cetuximab, a phenomenon whose mechanism needs further elucidation.

Mutational analysis. Sequence variants in the *EGFR* genes were observed in 6 of 25 NSCLC xenografts. In all these cases, the changes were either silent or represented intronic changes not considered to be functional. Mutations in *K-ras* and *p53* were detected in 6 of 25 (24%) and 13 of 25 (52%) of models, respectively. These data are consistent with previous reports on frequencies of mutations in these genes in NSCLC (33).

None of the *EGFR* or *p53* mutations investigated correlated alone or in combination with the response to anti-EGFR therapies. Interestingly, 5 of 6 tumors with *K-ras* mutations were resistant to erlotinib. However, the same *K-ras* mutation in codon 12 was associated with either sensitivity (ADC 7462) or resistance (PLC 7336) to anti-EGFR therapies.

Gene expression analysis. In total, RNA was isolated from 17 primary NSCLC specimens and from 2 to 5 vehicle control (PBS) tumors and hybridized to Affymetrix HGU133Plus2.0 arrays. High-quality gene expression data from the primary NSCLC specimen and the corresponding xenograft model derived thereof were available for 17 models and were used for a comparative analysis.

Unsupervised hierarchical clustering of samples (Fig. 2A) based on the expression of all genes revealed that 9 of the 17 primary tumors clustered directly with the xenografts derived thereof. These primary samples consisted of at least 25% tumor tissue. The other 8 xenografts formed a distinct cluster from primary tumors. Five of these primary tumors (SQC 7860, ADC 7406, ADC 7700, PLC 7064, and SQC 7177) contained <10% tumor tissue. We calculated the correlation coefficient between primary cancer and the xenograft derived thereof for all 17 cases. The correlation coefficient ranged between 0.945 and 0.782 with 10 of 17 > 0.900 indicating a high degree of similarity between the primary cancer and the corresponding xenograft model. The correlation coefficients are listed in Supplementary Table S1.

In all cases the xenograft tumors of one model clustered tightly together, showing high consistency between replicate tumors. A paired t test between the primary tumors and xenografts revealed 193 differentially expressed probe sets with $P < 10^{-7}$ (Supplementary Table S2). Clustering based on these 193 probe sets showed a clear distinction between primary tumors and xenografts (Fig. 2B), with most probe sets (155 of 193) being down-regulated in the xenograft models and only a very small number being up-regulated (38 of 193). The 193 probe sets correspond to 134 unique genes and main pathways represented in this data set were cell adhesion and immune response according to GeneGo Metacore pathway analysis (Supplementary Fig. S1).

We did a quantitative TaqMan PCR for one of the most strongly differentially expressed genes, the gene COL3A1, a collagen that is strongly expressed in connective tissue. We used primer/probe pairs specific for the human and the murine gene, respectively, and analyzed the gene expression level of the human and murine genes in the pairs of primary lung cancer and xenograft model derived thereof (Fig. 2C). For comparison, we measured expression levels of the housekeeping gene GAPDH. Human COL3A1 was detectable in the primary lung cancer but at much lower levels (higher CT values) in the xenograft samples. In contrast, the murine COL3A1 was strongly expressed in the xenografts but not in the primary lung cancer samples. Human GAPDH transcripts were strongly detectable in the primary tumors and the xenografts, whereas, as expected, the murine GAPDH was only expressed in xenograft samples. Moreover, results from control samples, mouse Lewis lung tumors, and human A549 lung cancer cells confirmed the species specificity of the TaqMan primer/probe pairs. In summary, this analysis shows that for the COL3A1 gene the results from global gene expression analysis are species specific; indeed, instead of human connective tissue, mouse stroma can be detected in the xenograft samples. Similar results were obtained when using primer/probe pairs specific for human and mouse COL1A2 and PECAM1 encoding for the CD31 vascular endothelial marker (data not shown).

Protein analyses. The protein expressions of EGFR, STAT1, STAT3, ERK, AKT, and PTEN as well as their corresponding phosphorylated forms were examined by immunoblotting in the 25 NSCLC xenograft models. Quantification of the immunoblots showed that the protein expression pattern of the 12 selected markers did not correlate with the response to the two EGFR-directed therapeutics. Individual, tumor-specific expression patterns were found for EGFR, ERK1, STAT1, STAT3, AKT, and the corresponding phosphorylated forms, whereas all tumors expressed similar high levels of PTEN (data not shown).

The analysis of xenograft tumors taken after 2 weeks of therapy with cetuximab or erlotinib compared with vehicle-treated controls revealed a down-regulation of the total EGFR content in 2 sensitive xenograft models (ADC 7462 and ADC 7466) of 6 analyzed. But in none of the resistant tumors investigated (exemplified for ADC 7387 and SQC 7343) a change in expression level was found (Fig. 3). In the xenograft model ADC 7462, additionally, a down-regulation of ERK1 after cetuximab treatment was observed. The other proteins, pEGFR, pSTAT1, pSTAT3, and pERK showed no regulation relating to sensitivity or resistance of the xenografts.

Discussion

NSCLCs are one of the most frequent tumor types, which present with a very bad prognosis and only minor therapeutic success had been made in the last years (34, 35). Therefore, an intensive search for better treatment modalities including

compounds targeting tyrosine kinases was initiated. Several clinical trials with therapies directed against the EGFR have been done (IDEAL, INTACT, and TALENT) showing a differential but in general not a promising outcome (36–39).

The outcome of these studies revealed an urgent need for a better stratification of patients. Thus far, no biomarker for prediction of response or outcome has been installed for routine use (40). One of the reasons may be that clinical samples used for the analysis of biomarkers were mainly pretreatment samples, and only available in minute amounts resulting in nonsufficient material for an extended study on the protein level. Further, clinical samples are relatively heterogeneous; they contain a variable percentage of cancer cells and other infiltrating cells.

NSCLC xenografts used thus far for therapeutic studies were derived mainly from established cancer cell lines (21). These cell lines have been cultivated for a long time in monolayers on plastic dishes and lost most of their original tumor tissue specificity. To circumvent these issues, we used a large panel of xenograft models that were established directly from patient-derived tumor specimens in immunodeficient mice. We (41) and others (42) have shown previously that colon cancer xenografts in early passages are very similar to the primary colon cancer from which they were derived with regard to histology, karyotype, and chemoresponsiveness.

Thus far, only few studies used patient-derived lung xenograft models (26–28). The study of Judde et al. (26) investigated the response of 5 xenograft models with wild-type EGFR to gefitinib in combination with cisplatin-based chemotherapeutic protocols. The study of Perez-Soler et al. (27) using NSCLC heterotransplants revealed similar engraftment rates (34 of 100) as ours. They also confirmed morphologic identity between original and transplanted tumors and showed a similar response rate to paclitaxel (21%) as we did (16%).

We were able to establish 25 routinely passagable NSCLC xenograft models starting from 102 NSCLC specimens. The engraftment rate of about 23% was in a similar range as the one reported by Cutz et al. (43) and is lower than the ones observed in our group for colon cancer xenografts with 43% (41) or acute lymphatic leukemias with 64% (44) but higher than for breast carcinomas with 9% (45). The NSCLC xenografts showed a high concordance with the corresponding clinical sample both concerning histology and immunohistologic staining for Ki-67 and EpCAM. Similar results of high comparativeness of xenografts with the original tumor were described by us (41) and others (27, 42, 46, 47).

The genome-wide RNA expression patterns of the clinical NSCLC specimens and the corresponding early-passage xenografts were analyzed by microarray analysis. In about half of the investigated cases (9 of 17), where global gene expression profiling data are available, the primary NSCLC specimens clustered together with the corresponding xenograft model (Fig. 2). The other 8 cases of primary lung cancers that clustered

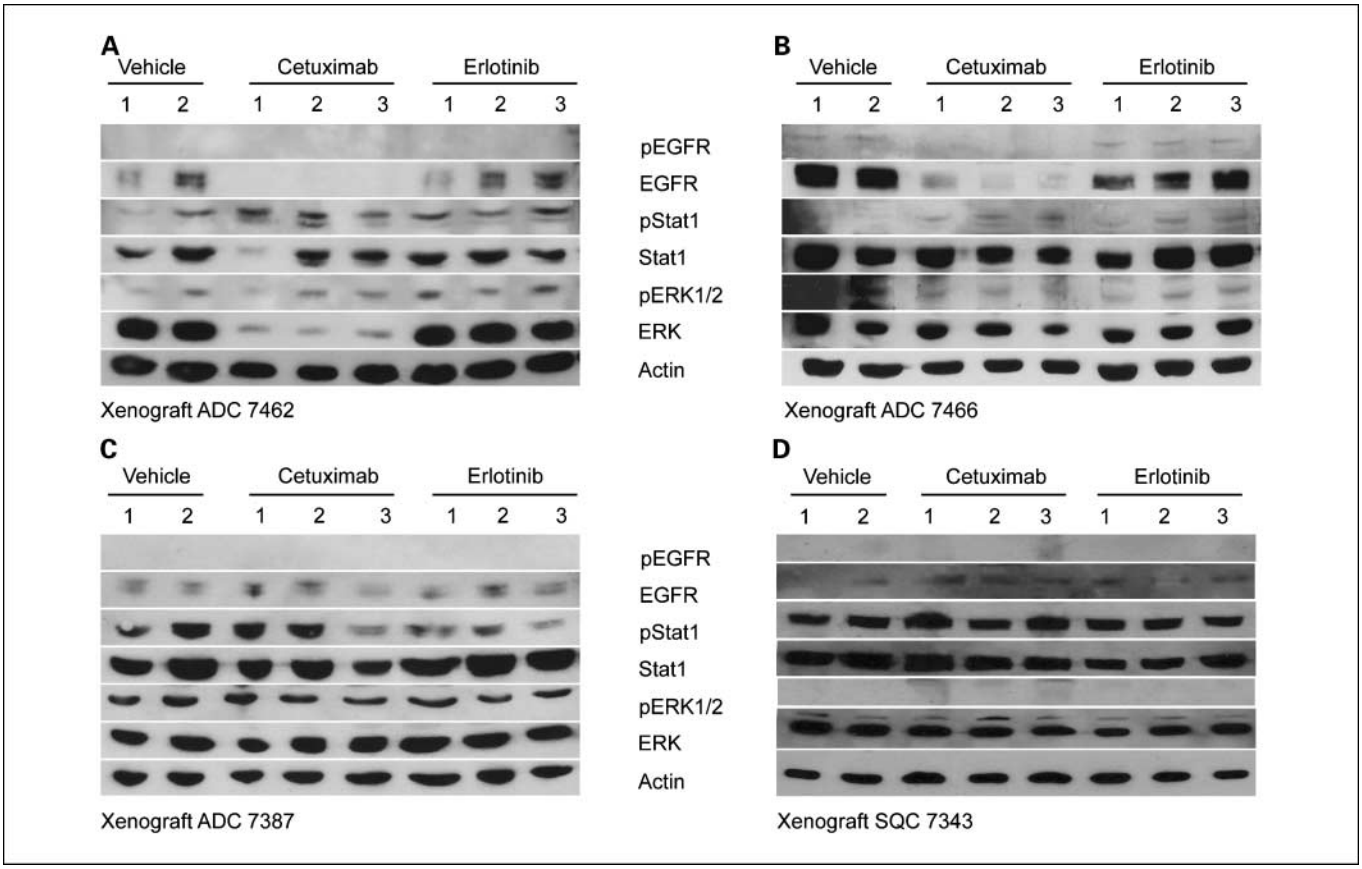

Fig. 3. Exemplified immunoblotting data of the proteins pEGFR, EGFR, pSTAT1, STAT1, pSTAT3, STAT3, pERK1/2, ERK, and β-actin as loading control. *A,* ADC 7462. *B,* ADC 7466 sensitive toward cetuximab and erlotinib. *C,* ADC 7387. *D,* SQC 7343 resistant toward cetuximab and erlotinib. Tumors were taken from the therapeutic experiments (described in Materials and Methods). Two samples each of vehicle treated and three samples each of cetuximab- or erlotinib-treated groups, respectively, were analyzed.

separately contained a lower amount of tumor cells in the clinical samples. However, the calculated correlation coefficients (Supplementary Table S1) showed a high concordance of gene expression of the xenografts with the corresponding clinical sample. We found 134 genes (<1% of the genome) that were differentially expressed between the clinical specimen and the xenograft derived thereof (Supplementary Table S2). In a similar genomic study with melanomas, a much lower correlation of only 75% with 1,374 differentially expressed genes between primary patient tumors and the corresponding xenografts was found (48). In the majority, the differentially expressed genes in our study belonged to the human stroma and immune cells, which are replaced during the early passaging by mouse tissue and are therefore not detected on the gene expression arrays that are specifically designed to detect human genes. This is also reflected by the fact that >80% of the differentially expressed genes are down-regulated in the xenografts compared to primary tumors.

The chemoresponsiveness of our panel of NSCLC xenografts revealed a relative sensitivity for paclitaxel, gemcitabine, and carboplatin, drugs that also give the highest response rates in the clinical situation (49). Most of our NSCLC donors were not chemotherapeutically pretreated so that no individual comparison of clinical and xenograft outcomes could be done. However, the differential responses of the 25 established xenografts to the single drug treatments (Tables 2 and 3) would highly justify an individual prediction of responsiveness.

In addition, we included cetuximab, a monoclonal antibody that binds to the extracellular domain of the EGFR, and erlotinib, a TKI in the chemosensitivity testing. Although in most of the published studies gefitinib was used for treatment, we decided for erlotinib as it has shown better antitumor effect in NSCLC (50).

The two therapies directed against the EGFR exerted a positive response (T/C values below 50%) in 12 of 25 and 6 of 25 of the xenografts, respectively (Table 3), although only in few cases a shrinkage of established tumors could be shown. Cetuximab treatment resulted in a stronger and dose-independent inhibition compared with erlotinib (Fig. 1C). Seven NSCLC xenograft models were remarkably growth inhibited by cetuximab but not by erlotinib (Table 3). The observed differential responsiveness of the xenograft models reflects the situation in the clinic: very few complete or partial responders and quite several intrinsically resistant NSCLC toward therapy with cetuximab have been reported (51). An individual prediction of responsiveness toward these therapies would therefore be highly warranted; thus far, no validated biomarkers have been developed for routine use.

Because the first description of mutations in the *EGFR* and a correlation with response to EGFR-targeted therapy (9, 52, 53), numerous investigations have been done to use this variable as prediction marker (8, 54, 55). It became obvious that mutations mainly arise in patients of Asian origin, females, nonsmokers, and adenocarcinomas, a cohort that also showed best responses to gefitinib (56). From these facts, it is not surprising that in our NSCLC xenograft collection originating from a Caucasian population with a low percentage of never smokers (1 of 25) and of both genders no relevant mutations in the *EGFR* gene were found. Independent of the lack of functional mutations, 12 of 25 xenografts were significantly growth inhibited by cetuximab and 6 of 25 xenografts by erlotinib pointing to the fact that other markers besides mutations in the target gene might determine therapeutic responsiveness. Our results agree with a report of Steiner et al. (57) that showed efficacy of cetuximab in several cell line-derived NSCLC xenograft models independent of mutations in the *EGFR*.

K-ras mutations have been described to cause intrinsic resistance toward TKI in NSCLC (55, 58–60). In our panel of NSCLC xenografts, 6 tumors presented with K-ras mutations from which 5 showed intrinsic resistance to erlotinib, confirming the reported observations. Only one xenograft with a *K-ras* mutation in codon 12 (ADC 7462) was highly responsive to both EGFR-targeted therapies. A 52% frequency of *p53* mutations found in our xenograft panel is comparable with the incidence of *p53* mutations in NSCLC patients (61). There was no correlation between *p53* mutations and therapeutic response. From these mutational analyses, it can be concluded in general that single gene alterations cannot alone or exclusively determine the sensitivity of a NSCLC toward an EGFR-targeted therapy.

To test the hypothesis that blocking the EGFR could result in changes of protein expression or phosphorylation status of the EGFR itself as well as downstream signal transduction proteins and as these changes might be pharmacodynamic markers, we studied protein expression of the EGFR signal transduction proteins in the xenograft models. We did not find a correlation between constitutive EGFR protein expression and response to EGFR-targeted therapies. Even after treatment, only minor changes were observed in accordance with drug response. Two tumors (ADC 7462 and ADC 7466) being sensitive to EGFR-targeted therapies showed a lower expression level of the EGFR protein after cetuximab and to a lower extent also after erlotinib treatment (Fig. 3). That reflects data reporting an internalization of EGFR protein after antibody treatment (62).

Whereas several preclinical studies did also not find a clear correlation between EGFR expression and gefitinib sensitivity (21, 63–65), others have reported a positive correlation (66). It was shown that NSCLC with high levels of phosphorylated AKT and mutated EGFR were more sensitive to gefitinib treatment and had a significantly longer time to progression and overall survival in advanced or metastatic stage (67–69). We were not able to confirm these results as in our models neither gain-of-function mutations in the EGFR nor constitutively active phosphorylated AKT correlated with treatment response. As potential reason for these partially conflicting results, the stage of our tumor samples should be considered. In many studies, advanced or metastatic NSCLC from patients or highly dedifferentiated cell lines have been used. In contrast, we included in our study exclusively primary tumors of patients diagnosed at early stages (T_2 and T_3) in which mutations of the EGFR or constitutively active downstream pathways (phosphoinositide 3-kinase or AKT) are rare events. Further, it is known that regulations of the EGFR protein only can be observed when high levels of ligands (e.g., EGF) are present. We suggest that, in contrast to cell culture experiments, *in vivo* physiologically only minor amounts of ligands are available, so that potential changes in protein expression are below the detection limit.

In summary, a large panel of well-characterized patient-derived NSCLC xenografts is now available whose

concordance with the clinical situation has been shown. These xenograft models allow to perform preclinical studies evaluating novel targeted therapies and uncovering the expression and regulation of biomarkers. Further investigations comparing the therapeutic response of NSCLC xenografts to the expression of resistance markers and growth factor ligands are ongoing and will be reported separately.

Disclosure of Potential Conflicts of Interest

I. Fichtner is employed by EPO-GMBH. The authors report no other conflicts.

Acknowledgments

We thank Diana Anders, Monika Becker, Sylvia Schulz, Martina Sperling, Sumarlin Lee, Diyanah Anuar, and Wen Lee Tan for excellent technical assistance.

References

1. Azim HA, Jr., Ganti AK. Targeted therapy in advanced non-small cell lung cancer (NSCLC): where do we stand? Cancer Treat Rev 2006;32:630–6.
2. Cappuzzo F, Finocchiaro G, Metro G, et al. Clinical experience with gefitinib: an update. Critical Rev Oncol Hematol 2006;58:31–45.
3. Blackhall F, Ranson M, Thatcher N. Where next for gefitinib in patients with lung cancer? Lancet Oncol 2006;7:499–507.
4. Dutta PR, Maity A. Cellular responses to EGFR inhibitors and their relevance to cancer therapy. Cancer Lett 2007;254:165–77.
5. Spicer J, Chowdhury S, Harper P. Targeting novel and established therapies for non-small cell lung cancer. Cancer Lett 2007;250:9–16.
6. Morgillo F, Lee HY. Resistance to epidermal growth factor receptor-targeted therapy. Drug Resist Updat 2005;8:298–310.
7. Özvegy-Laczka C, Cserepes J, Elkind NB, Sarkadi B. Tyrosine kinase inhibitor resistance in cancer: role of ABC multidrug transporters. Drug Resist Updat 2005;8:15–26.
8. Sharma SV, Bell DW, Settleman J, Haber DA. Epidermal growth factor receptor mutations in lung cancer. Nat Rev Cancer 2007;7:169–81.
9. Pao W, Miller VA. Epidermal growth factor receptor mutations, small-molecule kinase inhibitors, and non-small-cell lung cancer: current knowledge and future directions. J Clin Oncol 2005;23:2556–68.
10. Shigematsu H, Lin L, Takahashi T, et al. Clinical and biological features associated with epidermal growth factor receptor gene mutations in lung cancers. J Natl Cancer Inst 2005;97:339–46.
11. Kim KS, Jeong JY, Kim YC, et al. Predictors of the response to gefitinib in refractory non-small cell lung cancer. Clin Cancer Res 2005;11:2244–51.
12. Yang SH, Mechanic LE, Yang P, et al. Mutations in the tyrosine kinase domain of the epidermal growth factor receptor in non-small cell lung cancer. Clin Cancer Res 2005;11:2106–10.
13. Han SW, Kim TY, Jeon YK, et al. Optimization of patient selection for gefitinib in non-small cell lung cancer by combined analysis of epidermal growth factor receptor mutation, K-ras mutation, and Akt phosphorylation. Clin Cancer Res 2006;12:2538–44.
14. Bae NC, Chae MH, Lee MH, et al. EGFR, ERBB2, and KRAS mutations in Korean non-small cell lung cancer patients. Cancer Genet Cytogenet 2007;173:107–13.
15. Engelman JA, Zejnullahu K, Mitsudomi T, et al. MET amplification leads to gefitinib resistance in lung cancer by activating ERBB3 signaling. Science 2007;316:1039–43.
16. Engelman JA. The role of phosphoinositide 3-kinase pathway inhibitors in the treatment of lung cancer. Clin Cancer Res 2007;13:4637–40.
17. Chan SK, Gullick WJ, Hill ME. Mutations of the epidermal growth factor receptor in non-small cell lung cancer: search and destroy. Eur J Cancer 2006;42:17–23.
18. Han SW, Hwang PG, Chung DH, et al. Epidermal growth factor receptor (EGFR) downstream molecules as response predictive markers for gefitinib (Iressa, ZD1839) in chemotherapy-resistant non-small cell lung cancer. Int J Cancer 2005;113:109–15.
19. Cappuzzo F, Hirsch FR, Rossi E, et al. Epidermal growth factor receptor gene and protein and gefitinib sensitivity in non-small-cell lung cancer. J Natl Cancer Inst 2005;97:643–55.
20. Higgins B, Kolinsky K, Smith M, et al. Antitumor activity of erlotinib (OSI-774, Tarceva) alone or in combination in human non-small cell lung cancer tumor xenograft models. Anticancer Drugs 2004;15:503–12.
21. Helfrich BA, Raben D, Varella-Garcia M, et al. Antitumor activity of the epidermal growth factor receptor (EGFR) tyrosine kinase inhibitor gefitinib (ZD1839, Iressa) in non-small cell lung cancer cell lines correlates with gene copy number and EGFR mutations but not EGFR protein levels. Clin Cancer Res 2006;12:7117–25.
22. Huang S, Armstrong EA, Benavente S, et al. Dual-agent molecular targeting of the epidermal growth factor receptor (EGFR): combining anti-EGFR antibody with tyrosine kinase inhibitor. Cancer Res 2004;64:5355–62.
23. Raben D, Helfrich B, Chan DC, et al. The effects of cetuximab alone and in combination with radiation and/or chemotherapy in lung cancer. Clin Cancer Res 2005;11:795–805.
24. Zembutsu H, Ohnishi Y, Daigo Y, et al. Gene-expression profiles of human tumor xenografts in nude mice treated orally with the EGFR tyrosine kinase inhibitor ZD1839. Int J Oncol 2003;23:29–39.
25. Sirotnak FM. Studies with ZD1839 in preclinical models. Semin Oncol 2003;30:12–20.
26. Judde JG, Rebucci M, Vogt N, et al. Gefitinib and chemotherapy combination studies in five novel human non small cell lung cancer xenografts. Evidence linking EGFR signalling to gefitinib antitumor response. Int J Cancer 2007;120:1579–90.
27. Perez-Soler R, Kemp B, Wu QP, et al. Response and determinants of sensitivity to paclitaxel in human non-small cell lung cancer tumors heterotransplanted in nude mice. Clin Cancer Res 2000;6:4932–8.
28. Poupon MF, Arvelo F, Goguel AF, et al. Response of small-cell lung cancer xenografts to chemotherapy: multidrug resistance and direct clinical correlates. J Natl Cancer Inst 1993;85:2023–9.
29. Mountain CF. Revisions in the International System for Staging Lung Cancer. Chest 1997;111:1710–17.
30. Gross E, Kiechle M, Arnold N. Mutation analysis of p53 in ovarian tumors by DHPLC. J Biochem Biophys Methods 2001;47:73–81.
31. Chin TM, Anuar D, Soo R, et al. Detection of epidermal growth factor receptor variations by partially denaturing HPLC. Clin Chem 2007;53:62–70.
32. Ogino S, Kawasaki T, Brahmandam M, et al. Sensitive sequencing method for KRAS mutation detection by pyrosequencing. J Mol Diagn 2005;7:413–21.
33. Salgia R, Skarin AT. Molecular abnormalities in lung cancer. J Clin Oncol 1998;16:1207–17.
34. Shepherd FA. Chemotherapy for non-small cell lung cancer: have we reached a new plateau? Semin Oncol 1999;2:3–11.
35. Tiseo M, Franciosi V, Grossi F, Ardizzoni A. Adjuvant chemotherapy for non-small cell lung cancer: ready for clinical practice. Eur J Cancer 2006;42:8–16.
36. Bonomi PD, Buckingham L, Coon J. Selecting patients for treatment with epidermal growth factor tyrosine kinase inhibitors. Clin Cancer Res 2007;13:4606–12.
37. Thatcher N, Chang A, Parikh P, et al. Gefitinib plus best supportive care in previously treated patients with refractory advanced non-small-cell lung cancer: results from a randomised, placebo-controlled, multicentre study (Iressa survival evaluation in lung cancer). Lancet 2005;366:1527–37.
38. Maione P, Gridelli C, Troiani T, Ciardiello F. Combining targeted therapies and drugs with multiple targets in the treatment of NSCLC. Oncologist 2006;11:274–84.
39. Edelman MJ. An Update on the role of epidermal growth factor receptor inhibitors in non-small cell lung cancer. Semin Oncol 2005;32:3–8.
40. Baselga J, Arteaga CL. Critical update and emerging trends in epidermal growth factor receptor targeting in cancer. J Clin Oncol 2005;23:2445–59.
41. Fichtner I, Slisow W, Gill J, et al. Anticancer drug response and expression of molecular markers in early-passage xenotransplanted colon carcinomas. Eur J Cancer 2004;40:298–307.
42. Dangles-Marie V, Pocard M, Richon S, et al. Establishment of human colon cancer cell lines from fresh tumors versus xenografts: comparison of success rate and cell line features. Cancer Res 2007;67:398–407.
43. Cutz JC, Guan J, Bayani J, et al. Establishment in severe combined immunodeficiency mice of subrenal capsule xenografts and transplantable tumor lines from a variety of primary human lung cancers: potential models for studying tumor progression-related changes. Clinical Cancer Res 2006;12:4043–54.
44. Borgmann A, Baldy C, von Stackelberg A, et al. Childhood ALL blasts retain phenotypic and genotypic characteristics upon long-term serial passage in NOD/SCID mice. Pediatr Hematol Oncol 2000;17:635–50.
45. Fichtner I, Becker M, Zeisig R, Sommer A. *In vivo* models for endocrine-dependent breast carcinomas: special considerations of clinical relevance. Eur J Cancer 2004;40:845–51.
46. Fiebig HH, Dengler WA, Roth T. Human tumor xenografts: predictivity, characterization and discovery of new anticancer agents. In: Fiebig HH, Burger AM, editors. Relevance of tumor models for anticancer drug development. Contr Oncol Basel Karger 1999;54:29–50.
47. Whiteford CC, Bilke S, Greer BT, et al. Credentialing preclinical pediatric xenograft models using gene expression and tissue microarray analysis. Cancer Res 2007;67:32–40.
48. Xi Y, Riker A, Shevde-Samant L, et al. Global comparative gene expression analysis of melanoma patient samples, derived cell lines and corresponding tumor xenografts. Cancer Genomics Proteomics 2008;5:1–35.
49. Carney DN. Chemotherapy in the management of patients with inoperable non-small cell lung cancer. Semin Oncol 1996;23:71–5.
50. Shepherd FA, Rodrigues Pereira J, Ciuleanu T, et al. Erlotinib in previously treated non-small-cell lung cancer. N Engl J Med 2005;353:123–32.
51. Rosell R, Cuello M, Cecere F, et al. Treatment of non-small-cell lung cancer and pharmacogenomics: where we are and where we are going. Curr Opin Oncol 2006;18:135–43.
52. Lynch TJ, Bell DW, Sordella R, et al. Activating mutations in the epidermal growth factor receptor underlying responsiveness of non-small-cell lung cancer to gefitinib. N Engl J Med 2004;350:2129–39.

53. Paez JG, Janne PA, Lee JC, et al. EGFR mutations in lung cancer: correlation with clinical response to gefitinib therapy. Science 2004;304:1497–500.
54. Bell DW, Lynch TJ, Haserlat SM, et al. Epidermal growth factor receptor mutations and gene amplification in non-small-cell lung cancer: molecular analysis of the IDEAL/INTACT gefitinib trials. J Clin Oncol 2005;23:8081–92.
55. Eberhard DA, Johnson BE, Amler LC, et al. Mutations in the epidermal growth factor receptor and in KRAS are predictive and prognostic indicators in patients with non-small-cell lung cancer treated with chemotherapy alone and in combination with erlotinib. J Clin Oncol 2005;23:5900–9.
56. Konishi J, Yamazaki K, Kinoshita I, et al. Analysis of the response and toxicity to gefitinib of non-small cell lung cancer. Anticancer Res 2005;25:435–41.
57. Steiner P, Joynes C, Bassi R, et al. Tumor growth inhibition with cetuximab and chemotherapy in non-small cell lung cancer xenografts expressing wild-type and mutated epidermal growth factor receptor. Clin Cancer Res 2007;13:1540–51.
58. Pao W, Wang TY, Riely GJ, et al. KRAS mutations and primary resistance of lung adenocarcinomas to gefitinib or erlotinib. PLoS Med 2005;2:e17.
59. Miller VA, Zakoski M, Riely GJ, et al. EGFR mutation and copy number, EGFR protein expression and KRAS mutation as predictors of outcome with erlotinib in bronchioloalveolar cell carcinoma (BAC): results of a prospective phase II trial. J Clin Oncol 2006;24:364.
60. Massarelli E, Varella-Garcia M, Tang X, et al. KRAS mutation is an important predictor of resistance to therapy with epidermal growth factor receptor tyrosine kinase inhibitors in non-small cell lung cancer. Clin Cancer Res 2007;13:2890–6.
61. Viktorsson K, De Petris L, Lewensohn R. The role of p53 in treatment responses of lung cancer. BBRC 2005;331:868–80.
62. Sunada H, Magun BE, Mendelsohn J, et al. Monoclonal antibody against epidermal growth factor receptor is internalized without stimulating receptor phosphorylation. Proc Natl Acad Sci U S A 1986;83:3825–29.
63. Campiglio M, Locatelli A, Oliati C, et al. Inhibition of proliferation and induction of apoptosis in breast cancer cells by the epidermal growth factor receptor (EGFR) tyrosine kinase inhibitor ZD1839 ("Iressa") is independent of EGFR expression level. J Cell Physiol 2004;198:259–68.
64. Janmaat ML, Kruyt FA, Rodriguez JA, Giaccone G. Response to epidermal growth factor receptor inhibitors in non-small cell lung cancer cells: limited antiproliferative effects and absence of apoptosis associated with persistent activity of extracellular signal-regulated kinase or Akt kinase pathways. Clin Cancer Res 2003;9:2316–26.
65. Suzuki T, Nakagawa T, Endo H, et al. The sensitivity of lung cancer cell lines to the EGFR-selective tyrosine kinase inhibitor ZD1839 ("Iressa") is not related to the expression of EGFR or HER-2 or to K-ras gene status. Lung Cancer 2003;42:35–41.
66. Magne N, Fischel JL, Dubreuil A, et al. Influence of epidermal growth factor receptor (EGFR), p53 and intrinsic MAP kinase pathway status of tumor cells on the antiproliferative effect of ZD1839 ("Iressa"). Br J Cancer 2002;86:1518–23.
67. Capuzzo, F, Magrini, E, Ceresoli GL. Akt phosphorylation and gefitinib efficacy in patients with advanced non-small-cell lung cancer. J Natl Cancer Inst 2004;96:1133–41.
68. Sordella R, Bell DW, Haber DA, Settleman J. Gefitinib-sensitizing EGFR mutations in lung cancer activate anti-apoptotic pathways. Science 2004;305:1163–67.
69. Han SW, Kim TY, Hwang PG, et al. Predictive and prognostic impact of epidermal growth factor receptor mutation in non-small-cell lung cancer patients treated with gefitinib. J Clin Oncol 2005;23:2493–501.